EXPERIMENTAL ANALYSIS OF TRANSIENT PERFORMANCE OF THE DEW POINT LiCl PROBE

A.E. Attia

Mechanical Engineering Department, Faculty of Engineering,
Alexandria University, Alexandria, Egypt.

ABSTRACT

Theoretical analysis and experiments are performed to study the characteristic and performance of the dew point probe as well as its transient response with step variation in the condition of air. The probe is mainly made of Lithium chloride solution having 0.5 gm of the salt. The electrical resistance of LiCl solution is used as an inner heat generation to reactivate the solution and damp the adsorption mechanism of the water vapor. The experimental results of the probe temperature and concentration show that some initial oscillations experimentally occurred.

NOMENCLATURE

A_s	Area of solution as an electrical conductor; cm^2
A_{pr}	Probe surcumferential area; m^2
C	Concentration of solution by mass; kg LiC1/kg sol.
C′	Equivalent concentration; Equivalent/liter
C_{pr}	Specific heat of the probe; J/kg. K
D_v	Mass diffusivity; m^2/s
d_{pr}	Probe overall diameter; m
F_{db}	Time correction factor of dry bulb temperature; s
F_{dp}	Time correction factor of dew point temperature; s
F_u	The correction of air velocity
Gr_D	Grashof number; $d^3_{pr}\ \beta\ g\ (T_{pr}-T_{db})/\nu^2$
h	Heat transfer coefficient; $W/m^2.K$
h_D	Diffusion coefficient; m/s or $kg/(s.m^2.kg)/m^3$
h_{fg}	Heat of adsorption or evaporation; J/kg
K	Air thermal conductivity; W/m.K
K_p	Mass transfer coefficient; $kg/m^2.Pa$
l_s	Length of solution as an electric conductor; cm
m_{pr}	Mass of probe; kg
m_s	Mass of LiCl salt; kg
m_w	Mass of water in solution; kg
m_v	Mass of water vapor; kg
Nu_D	Nusselt number; $h\ d_{pr}/K$
P_{va}	Pressure of water vapor in air; Pa
P_{vp}	Pressure of water vapor in solution interface; Pa
Pr	Prandtl number; ν/α
Q_c	Convective heat transfer rate; W
Q_L	Heat rate of evaporation or adsorption; W
Q_v	Heat generation rate; W
Ra_D	Rayleigh number; $Gr_D.Pr$
Re_D	Reynolds number; $U.d_{pr}/\upsilon$
R_Ω	Electric resistance of solution; ohm
Sc	Shmidt number; α/D_v
Sh_D	Sherwood number; $h_D.d_{pr}/D_v$
T_{db}	Air dry bulb temperature; °C
T_{dp}	Air dew point temperature; °C
T_{pr}	Probe temperature; °C
t	Time; s
t^*	Basic probe response time; s
t^{**}	Actual probe response time; s
U	Air velocity; m/s
V	Applied voltage; volt
α	Air thermal diffusivity; m^2/s
β	Coefficient of thermal expansion; K^{-1}
υ	Kinematic viscosity; m^2/s
Λ	Specific electric conductivity of solution; cm^2/equivalent. ohm
ρ_Ω	Specific electric resistivity of solution; ohm.cm
φ	Lag parameter; $volt^2/W/K$

INTRODUCTION

In most of air conditioning applications specially the industrial ones such as spinning and weaving industry, the paper industry and the electronic production and assembly, the humidity control of the internal spaces and supply air is considered one of the important factors which determine the precision and the quality of the products.

Therefore, from the psychometric point of view, the air dew point measurement or control is a main determinant for the internal latent load or in other words the internal moisture gain. One of the dew point sensors, which can be accurately used, is the dewcel dew point probe, [1]. Letherman explained qualitatively the theory of operation of such probe, which depends on the high affinity of Lithium Chloride "LiCl" to adsorb the water vapor from the humid air. The interfacial film on the surface of the liquid desiccant has water vapor pressure less than the partial pressure of water vapor of the ambient air at the same temperature ref. [2,3,4,5]. The interfacial water vapor pressure of the solution increases as the solution temperature increases while it decreases as the solution concentration increases. In general, for a certain solution concentration there is a solution temperature at which the interfacial pressure becomes equal to the partial pressure of water vapor in the air. Therefore, it is obvious that for certain value of the air dew point there are a corresponding solution temperature and concentration in equilibrium. In order to obtain that temperature, heat should be added to the LiCl solution to damp the adsorption mechanism. The heat added in the probe is a heat generation depending on the electric resistance of the solution itself which increases with the increase of the solution concentration refs. [6,7,8]. Kostryko [9] studied the determinants which affect the dynamic properties of the probe. He considered that the concentration variation during the operation is negligible. In fact, this statement may lead to error about 7.5% in the normal range of operation. Sommer and Heinze [10] studied experimentally the gage defects of LiCl sensor. The study stated a strong nonlinear behavior due to solution decomposition. Error estimation was investigated by Mirtsch [11] due to the temperature difference and decomposition of solution. He also added a layer of $CaCl_2$ to prevent crust formation.

In the present work, the effect of the air dry bulb temperature, solution concentration, heat and mass transfer coefficients are considered as well as the effect of the applied electric voltage on the probe transient response in order to avoid the solution crystallization or liquification. Also the operating range of the probe is illustrated which is specified to prevent severe oscillatory behavior and insure reversible reactivation of the solution concentration.

THEORETICAL ANALYSIS

Figure (1) illustrates the energy balance performed on the probe in a certain time period dt. It is obvious that the probe has neither sensible nor latent heat effects on the environment to be measured. Upon this fact, all properties of the probe are considered time dependent only. The rate of change of lumped probe internal energy instantaneously balance with:-

1- The rate of convective heat transfer "Q_c" due to the temperature difference between the probe and the dry bulb temperature of the environmental air.
2- The rate of heat generation "Q_v" due to the electric resistance of the solution as an electrochemical effect.
3- The latent heat of evaporation or adsorption "Q_L" that is given by

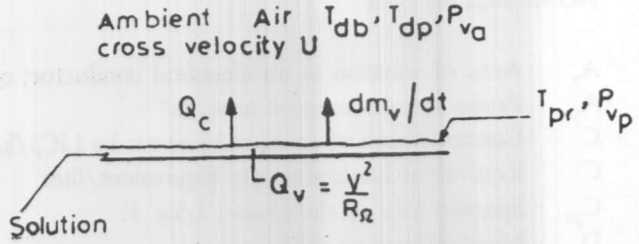

Figure 1. Interfacial energy balance.

$$Q_v - Q_c \pm Q_L = d\,(m_{pr}\, C_{pr}\, T_{pr})/dt \qquad (1)$$

The convective heat transfer term may represent natural or forced convection mechanisms according to the value of the air stream velocity "U". In general, the convective heat transfer can be calculated directly from;

$$Q_c = h\, A_{pr}\, (T_{pr} - T_{db}) \qquad (2)$$

The convective heat transfer coefficient "h" is obtained from the natural convection correlation:

$$Nu_D = n\, Ra_D^{\,m} \qquad (3\text{-a})$$

when the probe is used as a room sensor, while the coefficient is determined from the forced convection formula:

$$Nu_D = n\, Re_D^{\,m}\, Pr^{1/3} \qquad (3\text{-b})$$

as the probe is located as an air stream sensor. The values of m and n are obtained from refs. [5,12].

The heat generation term "Q_v" is found from:

$$Q_v = V^2 / R_\Omega \quad (4)$$

where

$$R_\Omega = \rho_\Omega l_s / A_s = \rho_\Omega * 0.54/6.07$$

and

$$\rho_\Omega = 1000 / \Lambda \; C'$$

The extension of Onsager's equation relates the equivalent electrical conductivity Λ of the monovalent salts in water with the salt equivalent concentration C' refs. [6,7,8] as,

$$\Lambda = \Lambda_o - (0.2238\ \Lambda_o + 50.49)\ C'^{1/2} + D' \quad (5)$$

where Λ_o is the equivalent conductivity at infinite dilution and D' is a correction factor depending on the equivalent concentration. In the operating range of mass concentration of 40% to 50%, it is found that the equivalent concentration equals to $8.10623 * 10^{-3}$ to $4.08567 * 10^{-3}$ cm^2/equivalent. ohm respectively.

The salt concentration "C'" in equivalent per one liter of water is related to the mass concentration "C" by

$$C = 42.397\ C' / (1000 + 42.397\ C') \quad (6)$$

where 42.397 gm is the equivalent mass of the LiCl as it is an monovalent salt.

The heat of evaporation term "Q_L" is proportional to the rate of mass of water vapor exchanged between the air and the interfacial film of LiCl solution, that

$$Q_L = \pm\ h_{fg} * dm_v/dt \quad (7)$$

The latent heat "h_{fg}" is function of the probe temperature and solution concentration ref. [2]. The rate of evaporation or adsorption is determined according to the water vapor pressure difference between the solution surface and the air to be measured that;

$$dm_v / dt = K_p\ A_{pr}\ (P_{vp} - P_{va}) \quad (8)$$

The mass transfer coefficient "K_p" is based on the difference in the vapor pressure. The relation between the diffusion coefficient "h_D" based on the density difference and "K_p" is directly obtained from;

$$K_p = h_D / R\ T_m \quad (9)$$

where "R" is the gas constant of water vapor and "T_m" is the average of the probe and air temperatures.

Upon "Colburn analogy", the diffusion coefficient "h_D" is obtained from;

$$Sh_D = n\ (Gr_D.Sc)^m \quad (10\text{-a})$$

for natural convection situation, while for forced convection, it is determined from;

$$Sh_D = n\ Re_D^{\ m}.Sc^{1/3} \quad (10\text{-b})$$

The values m and n are analogous to those of equations (3-a) and (3-b).

The value of the mass diffusivity "D_v" is calculated from the empirical equation for the water vapor in air ref. [5]; that

$$D_v = 0.926 * 10^{-3} * T_m^{2.5} / [P(T_m + 245)] \quad (11)$$

where P is the total pressure in Pa.

The solution concentration is subjected to successive variation with respect to time due to the rate of adsorption or evaporation. The solution concentration by mass is;

$$C = m_s / (m_s + m_w) \quad (12)$$

Since the amount of LiCl salt "m_s" is constant, and as ($dm_w/dt = - dm_v/dt$) the change of concentration is given by;

$$dC/dt = (C/m_s)\ dm_v/dt \quad (13)$$

The water vapor pressure of LiCl interfacial film "P_{vp}" is function of the solution temperature "T_{pr}" and the solution concentration "C" ref. [2]; i.e.

$$P_{vp} = f\ (T_{pr}, C)$$

In the present work, the data are collected from ref. [2,3,4], matched, and fed to the program routine as,

$$\ln (P_{vp}/P) = 11.775-[(3891+ 2.73 \times 10^3 C^2) /(T_{pr} + 232)] \quad (14)$$

The partial pressure of water vapor of the measured air "P_{vp}" is a function of the required dew point "T_{dp}" to be measured. The psychometric relation between them is obtained from ref. [5] and correlated in a program subroutine.

TECHNIQUE OF SOLUTION

Equation (1) is an unsteady nonlinear differential equation with initial value problem for the probe temperature "T_{pr}" since all terms are functions of the solution temperature and concentration. A time marching technique computer program routine is used with $\Delta t = 0.001$ sec. The dew point probe model is initially reset at a condition balanced with the humid air having a fixed condition at certain dry bulb and dew point temperatures. In order to study the probe response, a step variation in the air condition is done in the dry bulb or the dew point temperatures or in both of them. The program run is stopped when the final error in the probe temperature and the solution concentration becomes 0.01% related to the final steady state value. The response time t^* is obtained for basic initial condition ($T_{db}=24\ ^{o}C$, $T_{dp} = 16^{o}C$ and $U=5$ m/s).

The response times for other initial conditions t^{**} are determined and theoretically correlated to basic reference time t^* having the same step variations in dry bulb and dew point temperatures.

EXPERIMENTAL ARRANGEMENT

An experimental model is set up to verify the theoretical model results of performance and response. Figure (2-a) illustrates the details of the dew point sensor used while Figure (2-b) shows the experimental arrangement and measurements. The probe consists of T-type (copper-constantan) thermocouple of AWG-24. The thermocouple is inserted in a glass tube through a Tin socket molten inside the glass to insure good temperature distribution of the probe. The glass tube has an outside diameter of 3.5 mm and a thickness of 1.1 mm. Two electric platinum wires are winded on the tube separated by multi-layer of wicked cloth of 3.1 mm total thickness. The wicked cloth is used as a medium to suspend the LiCl solution. The effective overall outside diameter is 9.6 mm while its active length is 28.1 mm.

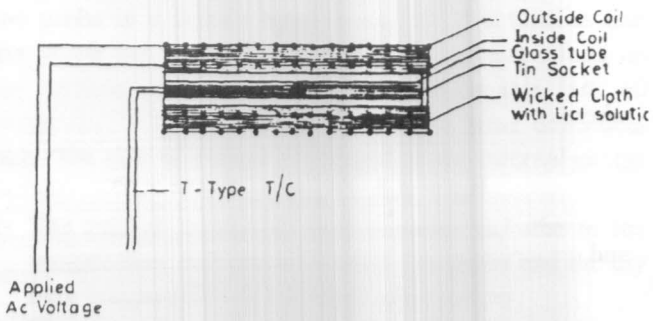

Figure 2-a. Probe sensor.

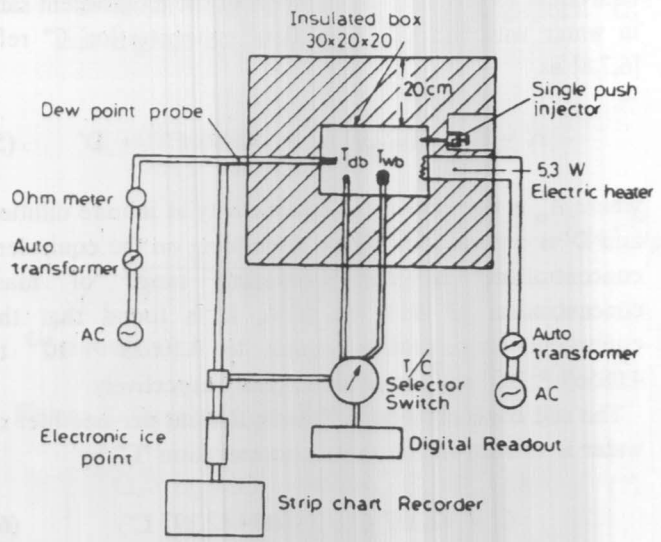

Figure 2-b. Experimental arrangement.

The probe heat capacity "$m_{pr}\ C_{pr}$" in RHS of equation (1) could be calculated as a lumped model from the heat capacities of the individual components of the probe constructed in Figure (2-a), i.e. the platinum wire, the wick cloth, the glass tube and the LiCl solution; that

$$m_{pr}\ C_{pr} = (mC)_{pw}+(mC)_{clo}+(mC)_{gl}+(mC)_{sol} \quad (15)$$

The specific heat of the wire "C_{pw}" wick cloth "C_{clo}" and glass "C_{gl}", obtained from ref. [13], are equal to 133, 1289 and 800 j/kg. k respectively while their masses m_{pw}, m_{clo} and m_{gl} are 0.44, 0.26 and 0.27 gm. The specific heat of the LiCl solution is correlated from ref. [2] as a function of concentration; that

$$C_{sol} = 3940 - 3140\ C \text{ j/kg.k} \quad (16)$$

The value of C_{sol} is accurate in the range 40% to 50% mass concentration.

The probe is used to measure the air condition inside a 20 cm thickness insulated box having inside dimensions of 30 * 20 * 20 cm. The box is used as an artificial environment insulated from the thermal external disturbance. The step variation is made using a 5.3 W electric heater and a single push sprayer injector. The air condition inside the box is sensed with two T-type thermocouples: one as dry bulb and the other as wet bulb thermometer. The wet bulb temperature thermocouple is embedded in tin/glass bulb covered with wetted cloth. The thermocouples are connected to digital temperature readout via selector switch. The readout has a resolution of 0.1 °C and contained a built-in self ice point compensation. The probe temperature or in other words the solution temperature "T_{pr}" is simulated on a strip chart recorder with 0.01 °C resolution through an electronic ice point reference. The electric resistance of the solution which is a function of the solution concentration is measured and simulated on an ohm-meter as a concentration recorder. The AC voltage applied to the probe solution is fixed at a certain value using an auto-transformer. The test run starts with setting the probe in the box by applying a suitable AC voltage normally 10-16 volts with natural convection situation. When the solution temperature "T_{pr}" and the electric resistance become constants, the probe is suddenly subjected to very short "10 s" heat addition using the electric heater and moisture addition using the injector inside the box, meanwhile the strip chart starts to record the transient response of the probe temperature while the solution electric resistance is registered. The experimental results are obtained to determine the experimental probe performance and the transient response for variation in the environmental air dry bulb or dew point temperatures, or both.

RESULTS AND DISCUSSIONS

Figures (3-a) and (3-b) represent the performance curves of the present dew point probe. They are used to simulate the dew point and dry bulb temperatures of the air using the corresponding measured parameters (the probe temperature and the electric resistance of the LiCl). It is found experimentally that the solution concentration should be limited to 50% maximum and 40% minimum to prevent solution crystallization or liquification in case of the severe oscillatory performance. The term $\varphi = V^2/hA_{pr}$ is considered an important parameter balancing the heat generation with the convective heat from the probe. Experimentally, it is recommended to operate the probe at a range of φ from 20,000 to 30,000. The smaller values of φ increase the response time and liquify the solution while the higher values increase the oscillatory behavior of the probe temperature and LiCl concentration as well as crystallize the salt. Figure (3-a) illustrates that as the solution electric resistance (or concentration) increases, a higher probe temperature is required to balance with a certain value of air dew point to achieve zero water vapor pressure potential between the solution interface and air inside the box. Figure (3-b) is used to obtain the steady state temperature potential between the probe and the dry bulb temperature of air i.e. a balance between the heat generation and the convective heat from the probe to air.

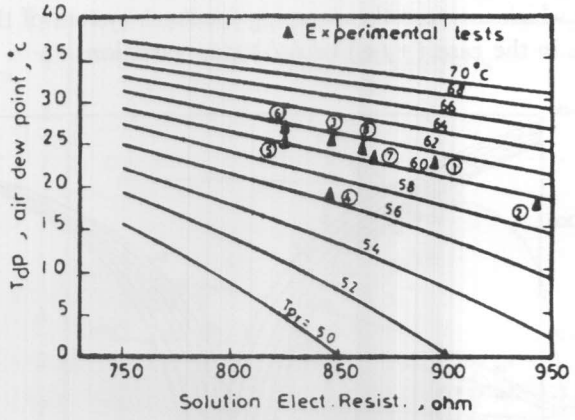

Figure 3-a. Air dew point temperature versus solution electric resistance.

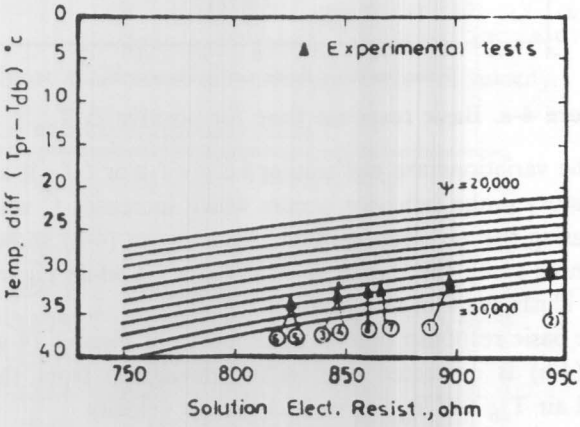

Figure 3-b. Solution and air dry bulb temperature potential versus solution electric resistance.

The probe basic response time is illustrated in Figures (4-a) and (4-b) for positive and negative ΔT_{dp} respectively. The figures are based on a fixed air initial condition of 24°C dry bulb temperature and 16°C dew point temperature as well as an air velocity of 5 m/s with $\varphi = 28{,}000$. The theoretically obtained basic response time t^* is subjected to three theoretical correction factors depending on the air initial condition and air velocity deviated from the aforenamed values. The figures show that t^* increases as positive or negative ΔT_{db} decreases. Also the figures illustrated that in the positive-to-positive (+/+) or negative-to-negative (-/-) step variation in dry bulb and dew point temperatures, the response time increases as ΔT_{dp} increases. The response time t^* decreases as ΔT_{dp} decreases in case of (+/-) or (-/+) conditions. The difference between the two trends can be explained when considering the fact that the increase in the T_{db} or T_{dp} requires higher probe temperature and vise versa which increase the damping feedback system of the probe in the case (+/+) or (-/-) step variation.

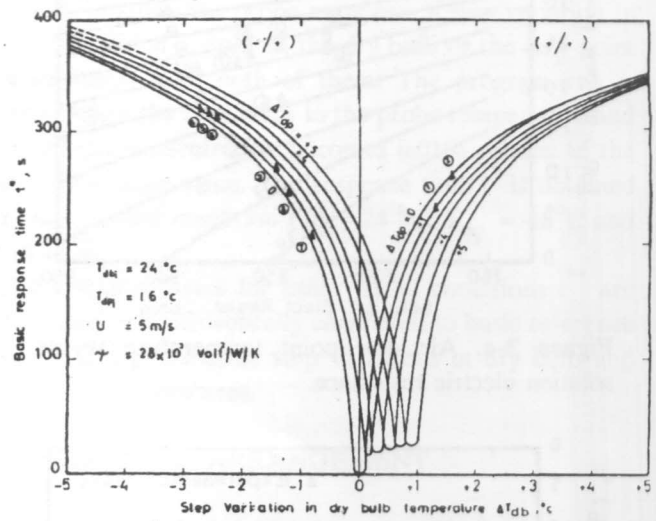

Figure 4-a. Basic response time for positive ΔT_{dp}.

If the variations are not similar i.e. (+/-) or (-/+), an oscillatory probe behavior occurs which increases t^* with increasing the variation amount. Also Figure (4-a) shows minimum t^* in the range $0 < \Delta T_{db} < +1$ while Figure (4-b) illustrates that minimum at $0 > \Delta T_{db} > -1$.

The basic response time t^* obtained from Figures (4-a) and (4-b) is corrected due to the deviations from the initial air T_{db} and T_{dp} as well as the air velocity.

Inspection of the theoretical results of 576 computer runs recapitulates the relation between the basic response time t^* and the actual theoretical response time t^{**} as follows;

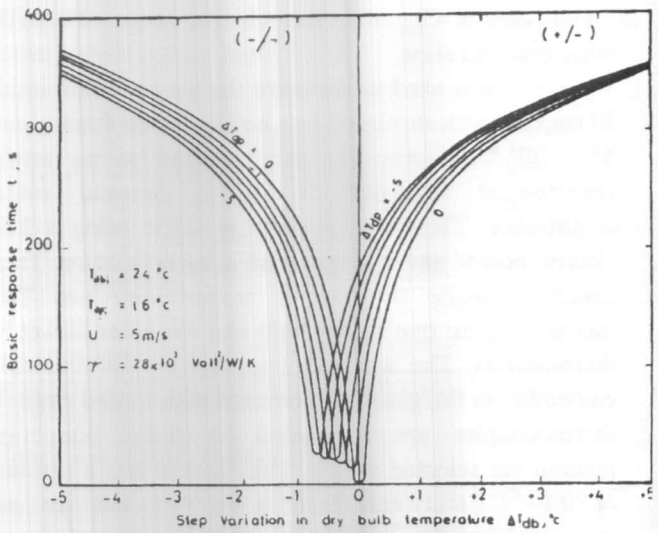

Figure 4-b. Basic response time for negative ΔT_{dp}.

$$t^{**} = (t^* + F_{db} + F_{dp}).\ F_u \qquad (17)$$

The time correction factor F_{db} due to the initial T_{dbi} depends only on the step variation in T_{db} and is theoretically obtained as;

$$F_{db} = -1.6\ (T_{dbi} - 24)\ ,\ s\ \Delta T_{db} = \pm 1\ ^{\circ}C$$

$$F_{db} = -2.2\ (T_{dbi} - 24)\ ,\ s\ \Delta T_{db} = \pm 2\ ^{\circ}C$$

$$F_{db} = -2.5\ (T_{dbi} - 24)\ ,\ s\ \Delta T_{db} = \pm 3\ ^{\circ}C$$

$$F_{db} = -2.8\ (T_{dbi} - 24)\ ,\ s\ \Delta T_{db} = \pm 4\ ^{\circ}C$$

$$F_{db} = -3.1\ (T_{dbi} - 24)\ ,\ s\ \Delta T_{db} = \pm 5\ ^{\circ}C \qquad (18)$$

The set of equations (18) shows that F_{db} increases as the step variation increases. Also it illustrates that the actual response time decreases as the initial dry bulb temperature increases. The interpolation between the coefficients could be used without noticeable error.

Figure (5) is used to correct the response time according to the initial dew point temperature. The value of f_{dp} is obtained as a function of ΔT_{db} and ΔT_{dp} The time correction factor F_{dp} is directly determined as.

$$F_{dp} = f_{dp}\ (T_{dpi} - 16),\ s \qquad (19)$$

For no step variation in the dry bulb temperature;

$$F_{dp} = [-4.5 - 2.5\ |\ \Delta T_{dp}\ |]\ (T_{dpi} - 16)\ ,\ s \qquad (20)$$

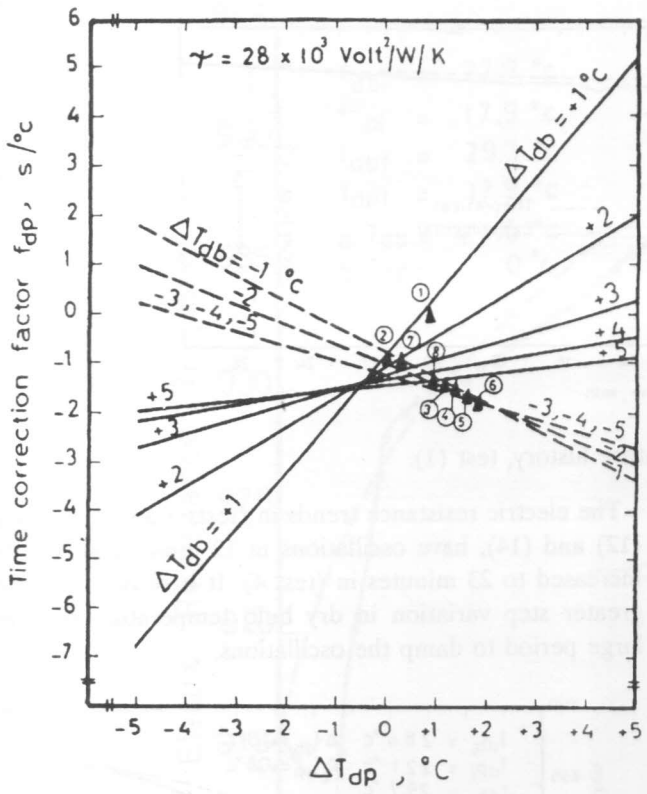

Figure 5. Theoretical correction factor of initial T_{dp}.

The third correction factor F_u obtained from Figure (6) constructed at $\varphi = 28000$ is used when the air velocity deviates from 5 m/s. It is found that F_u depends on the velocity "U" and the amount of step variation of dew point temperature ΔT_{dp}. The step variation in the dry bulb temperature has a negligible effect on F_u. However, if the air velocity decreases, the heat and mass transfer coefficients decrease and therefore, the applied electric voltage should be decreased and vise versa.

Table (1) compares between the theoretical and experimental results. The theoretical basic response time t^{*} is determined from Figures (4-a) and (4-b) according to the values of ΔT_{db} and ΔT_{dp}. The theoretical response time t^{**} is found using the theoretical correction factors F_{db}, F_{dp} and F_u obtained from equation (18), Figure (5) and Figure (6) respectively. Inspection of comparisons between the theoretical and experimental results shows that the percentage error ranges from 3.18 to 8.64%. Also it is found that the error increases as the step variation in the dew point temperature increases. The results illustrate that the response time of a probe, located in a environment of air having zero velocity, increases to a value of 34 minutes. It is obvious, that the low heat and mass transfer coefficients between the sensor and the stagnant air have the great influence in increasing the transfer lag of the probe response time.

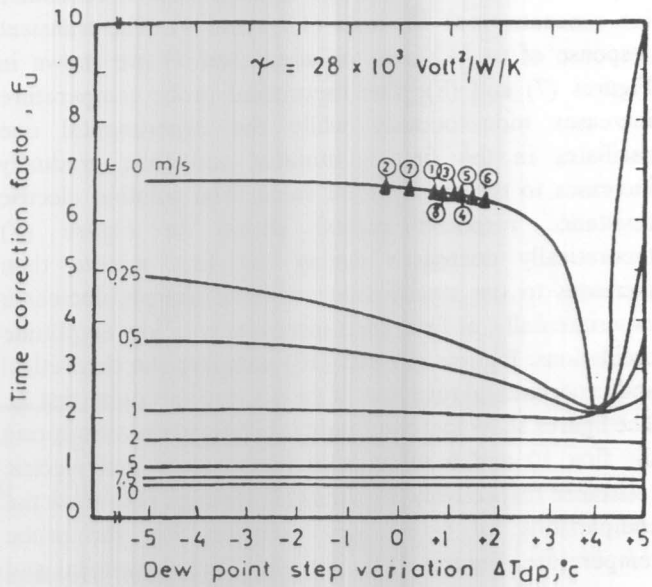

Figure 6. Theoretical correction factor of velocity.

Table 1. Comparison between theoretical and experimental results.

Test NO	T_{dpi}	T_{dpf}	T_{dpf}	T_{dpf}	t^{*}	F_{dp}	F_{dp}	F_u	t^{**} Theo.	t^{**} Exp.	Error %
1	28.4	22.1	29.7	22.9	235	-7.832	-0.305	6.55	1486	1536	3.36
2	22.7	17.9	29.3	17.9	262	-7.252	-1.805	6.60	1669	1722	3.18
3	29.6	24.1	28.2	25.3	264	-10.30	-12.15	6.45	1558	1614	3.59
4	26.2	17.1	23.5	18.4	320	-5.302	-1.705	6.45	2018	2092	3.67
5	29.3	23.9	26.7	25.4	317	-12.61	-12.64	6.40	1867	1994	6.80
6	30.1	24.8	26.7	26.6	312	-14.15	-15.40	6.35	1794	1951	8.76
7	28.6	22.8	27.8	23.1	205	5.888	-16.121	6.57	1268	1309	3.23
8	29.1	22.9	27.9	23.8		-8.772	-8.970	6.50	1477	1528	3.45

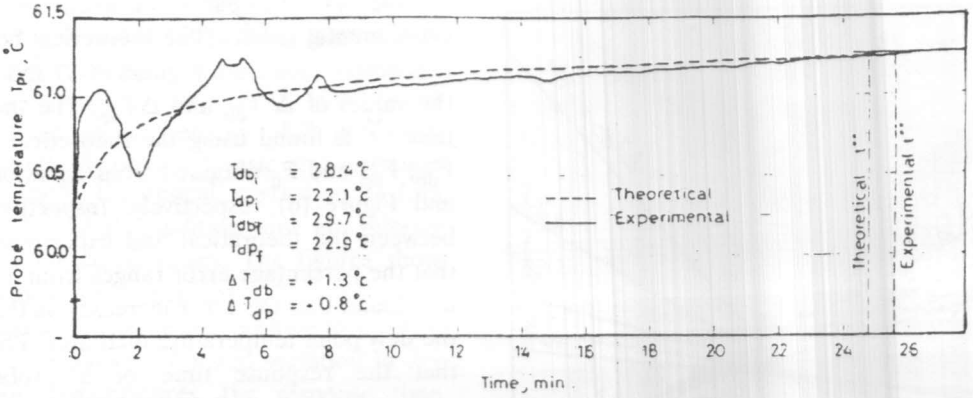

Figure 7. Probe temperature history, test (1).

Figures (7) through (14) illustrate the comparison between the theoretical and experimental transient period of probe temperature and the solution electric resistance (or concentration) for tests (1,2,3 and 4). The transient response of (+/+) step variation (test 1) are shown in Figures (7) and (8). The theoretical probe temperature increases monotonously while the experimental one oscillates in the first 8 minutes and then gradually increases to the steady state value. The solution electric resistance response period shown in Figure (8) theoretically decreases during the first minute then increases to the steady value while it sharply decreases experimentally, at first, then increases with low amplitude oscillations. Figures (9) and (10) compare the theoretical and experimental response of (+/0) step variation (test 2). The figures show low amplitude oscillatory behavior during the first 10 and 6 minutes in temperature and electric resistance respectively. Figures (11) through (14) show the comparisons for (-/+) step variation. For the probe temperature, Figures (11), and (13), the theoretical and experimental results have the same trend except initial oscillation in the experimental values during 8 minutes in (test 3) extended to 20 minutes in (test 4).

The electric resistance trends in (tests 3 and 4), Figures (12) and (14), have oscillations in 12 minutes in (test 3) increased to 23 minutes in (test 4). It is obvious that the greater step variation in dry bulb temperature requires large period to damp the oscillations.

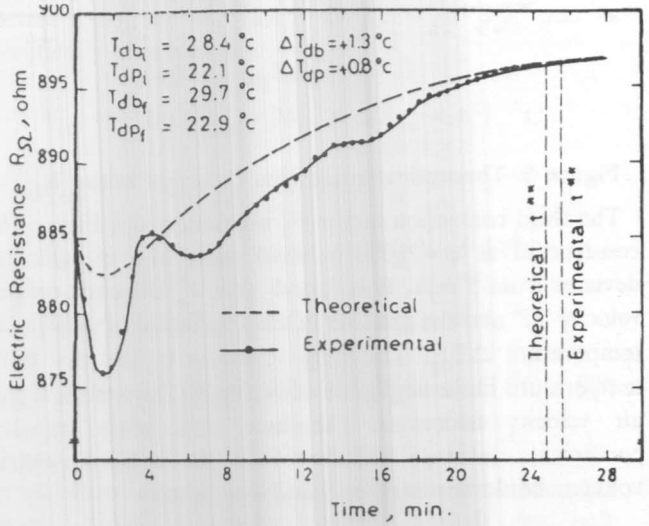

Figure 8. Solution electric resistance history, test (1).

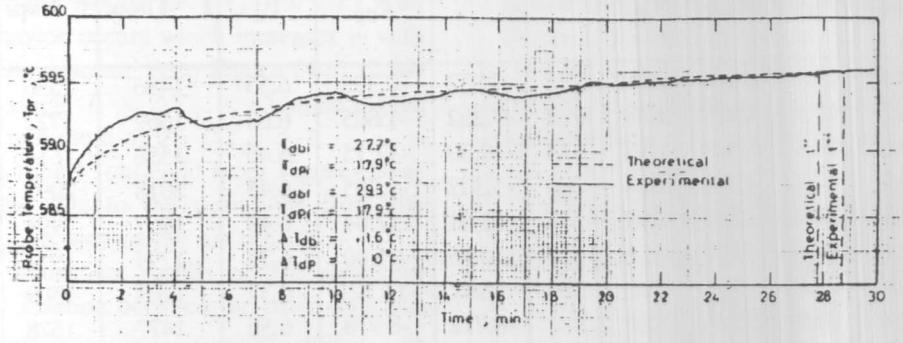

Figure 9, Probe temperature history, test (2).

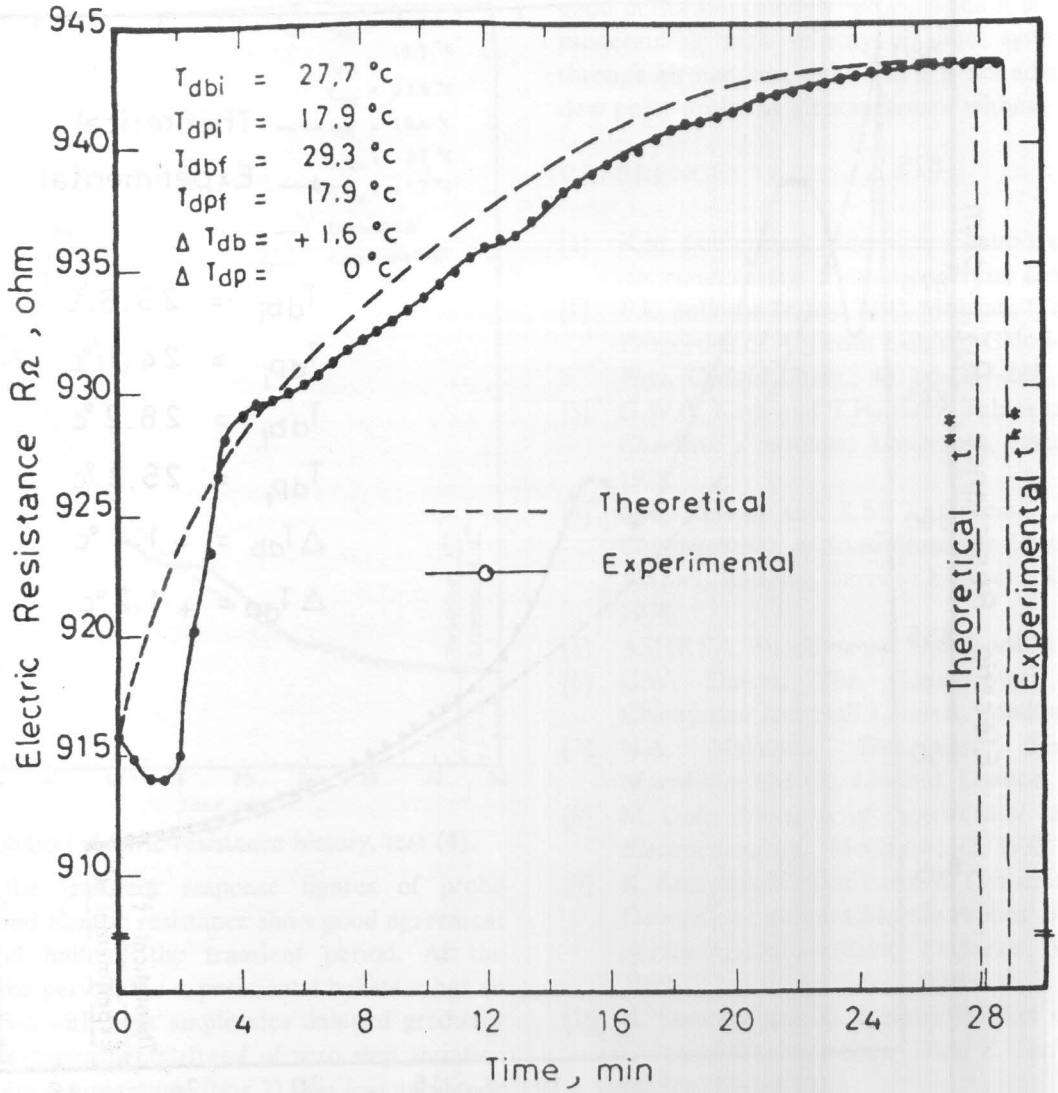

Figure 10. Solution electric resistance history, test (2).

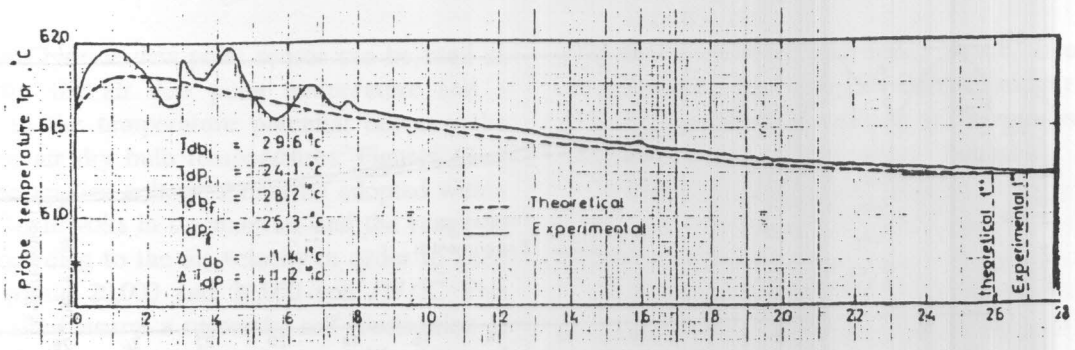

Figure 11. Probe temperature history, test (3).

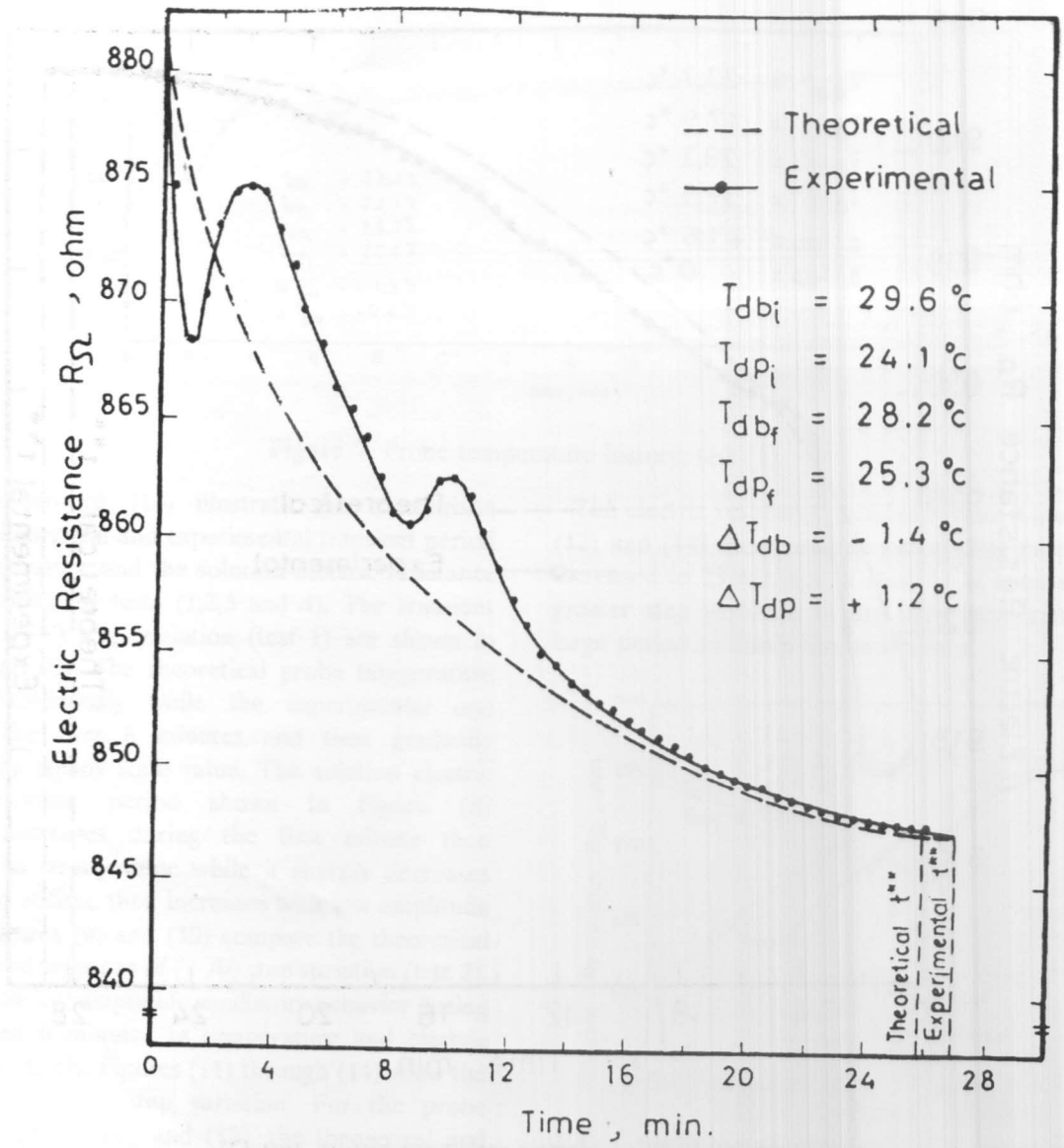

Figure 12. Solution electric resistance history, test (3).

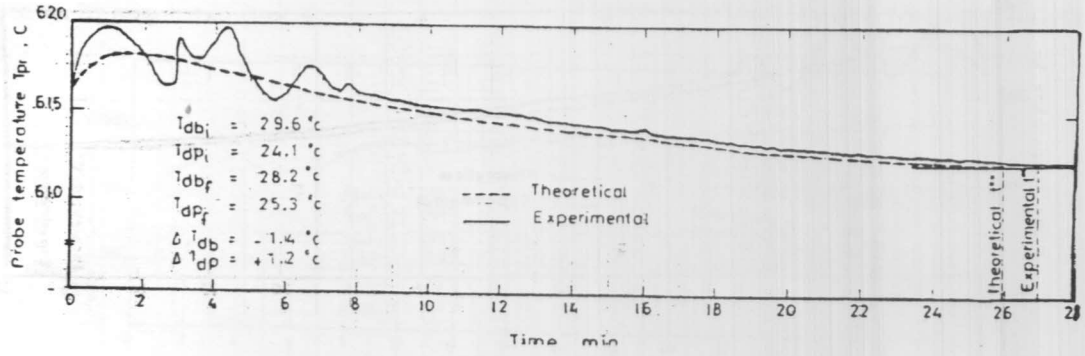

Figure 13. Probe temperature history, test (4).

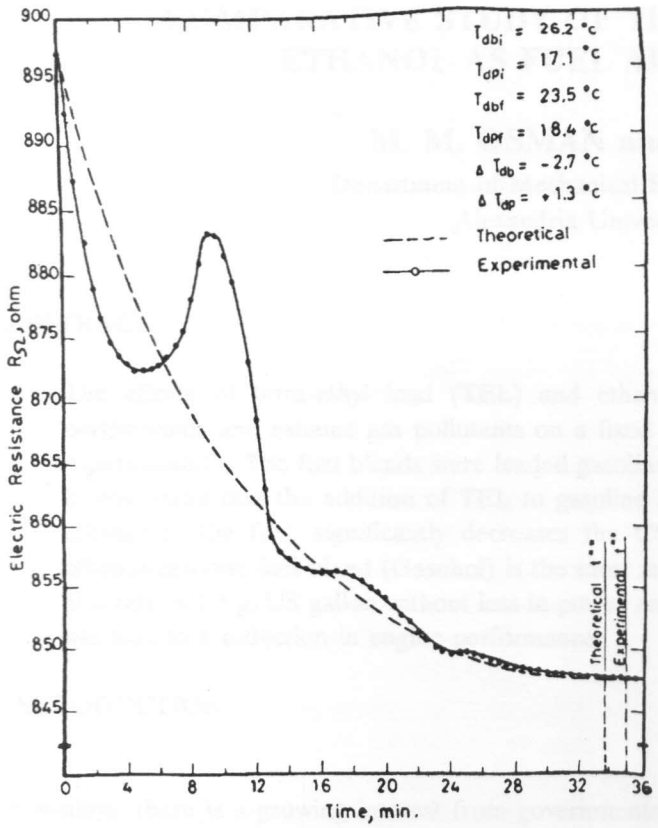

Figure 14. Solution electric resistance history, test (4).

Generally, the transient response figures of probe temperature and electric resistance show good agreement at the second half of the transient period. At the beginning of the period, the experimental behavior has an oscillatory trend with high amplitudes damped gradually with time. The experimental trend of zero step variation in the dew point temperature, (test 2), has low amplitude but the damping period increases.

CONCLUSIONS

The Lithium Chloride dew point sensor can be used as a simulator for the air dew point temperature and a compensator to the temperature potential between the probe and the air dry bulb temperatures, Figures (3-a) and (3-b). The applied voltage should be adopted within the range 10 to 16 volts in stagnant air and the range 30 to 50 volts according to the air velocity in order to keep the term φ within 20,000 and 30,000 volt^2/W/K. This range of operation insures a successful self reactivation of the probe solution and prevents the crystallization and liquification of solution. The study of the probe performance states that the probe transfer lag is minimized when the air velocity increases which implies a good performance of the probe when it is connected to a moderate or high velocity air duct system as well as through air handling units and it is not advised to use the dew point probe as a room sensor without sample fan.

REFERENCES

[1] K.M. Letherman, *Automatic Controls of Heating and Air conditioning*. Pergamon Press, London, 1981.

[2] F.E. Johnson Jr. and M.C. Molstad, "Thermodynamic Properties of Aqueous Lithium Chloride Solution" *J. Phys. Colloid Chem.*, 44, pp. 257-281, 1951.

[3] G.W.C. Kaye and T.H. Laby, Tables of *Physical and Chemical Constants*, Longmans, London, 14th ed., 1973.

[4] M.F. Leviers and K.M. Letherman, *The Extension Characteristics of Some Materials Used for Humidity Sensors*, Building, Services Engineer, 45, pp. 205-210, 1978.

[5] ASHREA, *Fundamental Handbook*, 1989.

[6] C.W. Davies, *The Conductivity of Solutions*, Champman and Hall Limited, London, 1933.

[7] N.A. Mckenna, *Theoretical Electrochemistry*, MacMillan and Co. Limited, London, 1984.

[8] M. Dole, *Principles of Experimental and Theoretical Electrochemistry*, McGraw-Hill, 1933.

[9] K. Kostyrko, "Optimization of Dynamic Properties of Dew-point Lithium Chloride Probes", *J. of Institution of Heating and ventilating Engineers*, 37, pp. 159-167, 1969.

[10] K. Sommer and D. Heinze, "Defect of the Lithium Chloride Moisture Gage" *Wiss. Z.-Tech. Hochsch*, 26 (4), pp. 69-74, 1980.

[11] F. Mirtsch and N. Frank, "Development and Investigation of A Modified Lithium Chloride Heated Electrical Hygrometer" *TM. Tech. Mess*, 47 (5), pp. 181-185, 1980.

[12] E.R.G. Eckert and R.M. Drake, *Heat and Mass Transfer*, McGraw-Hill Book Company, 1982.

[13] K. Raznjevic, *HandBook of Thermodynamic Tables and Charts*, Hemisphere Publishing Corporation, 1976.